doi:10.1093/brain/aww313 BRAIN 2017: 140; 457–471 | 457

BRAIN
A JOURNAL OF NEUROLOGY

Focal temporal pole atrophy and network degeneration in semantic variant primary progressive aphasia

Jessica A. Collins,[1] Victor Montal,[2] Daisy Hochberg,[1] Megan Quimby,[1] Maria Luisa Mandelli,[3] Nikos Makris,[4] William W. Seeley,[3,5] Maria Luisa Gorno-Tempini[3] and Bradford C. Dickerson[1]

A wealth of neuroimaging research has associated semantic variant primary progressive aphasia with distributed cortical atrophy that is most prominent in the left anterior temporal cortex; however, there is little consensus regarding which region within the anterior temporal cortex is most prominently damaged, which may indicate the putative origin of neurodegeneration. In this study, we localized the most prominent and consistent region of atrophy in semantic variant primary progressive aphasia using cortical thickness analysis in two independent patient samples ($n = 16$ and 28, respectively) relative to age-matched controls ($n = 30$). Across both samples the point of maximal atrophy was located in the same region of the left temporal pole. This same region was the point of maximal atrophy in 100% of individual patients in both semantic variant primary progressive aphasia samples. Using resting state functional connectivity in healthy young adults ($n = 89$), we showed that the seed region derived from the semantic variant primary progressive aphasia analysis was strongly connected with a large-scale network that closely resembled the distributed atrophy pattern in semantic variant primary progressive aphasia. In both patient samples, the magnitude of atrophy within a brain region was predicted by that region's strength of functional connectivity to the temporopolar seed region in healthy adults. These findings suggest that cortical atrophy in semantic variant primary progressive aphasia may follow connectional pathways within a large-scale network that converges on the temporal pole.

1 Department of Neurology, Massachusetts General Hospital/Harvard Medical School, Charlestown, MA, USA
2 Department of Neurology, Institut d'Investigacions Biomèdiques Sant Pau-Hospital de Sant Pau, Universitat Autònoma de Barcelona, Barcelona, Spain
3 Department of Neurology, University of California at San Francisco, San Francisco, CA, USA
4 Department of Psychiatry, Massachusetts General Hospital/Harvard Medical School, Charlestown, MA, USA
5 Department of Pathology, University of California at San Francisco, San Francisco, CA, USA

Correspondence to: Dr Jessica A. Collins
MGH Frontotemporal Disorders Unit
149 13th Street Charlestown, MA, 02129,
USA
E-mail: jcollins21@mgh.harvard.edu

Correspondence may also be addressed to: Dr Bradford C. Dickerson. E-mail: brad.dickerson@mgh.harvard.edu

Keywords: atrophy; resting state connectivity; primary progressive aphasia; semantic dementia; temporal lobe

Abbreviations: rs-fcMRI=resting-state functional connectivity MRI; svPPA = semantic variant primary progressive aphasia

Received March 28, 2016. Revised August 10, 2016. Accepted October 25, 2016. Advance Access publication December 30, 2016

Introduction

The semantic variant of primary progressive aphasia (svPPA) is a devastating, ultimately fatal, neurodegenerative disease characterized by the progressive loss of semantic memory (Warrington, 1975; Snowden *et al.*, 1989; Hodges *et al.*, 1992; Hodges and Patterson, 2007; Gorno-Tempini *et al.*, 2011). A wealth of neuroimaging studies have identified an extensive pattern of asymmetric bilateral cortical and subcortical neurodegeneration in svPPA, which is most prominent in the left anterior temporal cortex and encompasses a large portion of the temporal lobes (reviewed in Whitwell and Josephs, 2012; Diehl-Schmid *et al.*, 2014). As svPPA progresses, the pattern of atrophy observed becomes more distributed, and envelops inferior frontal, anterior insular, anterior cingulate, posterior temporal, and parietal cortex (Czarnecki *et al.*, 2008; Brambati *et al.*, 2009, 2015; Rohrer *et al.*, 2009), as well as the ventral striatum and amygdala. SvPPA is usually considered to be a subset of individuals with semantic dementia (Adlam *et al.*, 2006), which has a heterogeneous clinical presentation including impairments in language, visual knowledge, multimodal semantic memory, and social cognition and behavioural regulation (Chan *et al.*, 2009; Josephs *et al.*, 2009). Whereas a proportion of patients meeting the criterion for semantic dementia (~30%) present initially with atrophy that is more pronounced in the right than left anterior temporal lobes (Chan *et al.*, 2009; Josephs *et al.*, 2009), svPPA is always associated with early atrophy that is most pronounced in the left anterior temporal lobe. Here, we chose to focus on patients meeting the criteria for svPPA (Gorno-Tempini *et al.*, 2011), which emphasizes predominant semantic language impairment and left anterior temporal atrophy.

The localization of the most prominent neurodegeneration (as measured by atrophy or hypometabolism) in svPPA, which may indicate the putative origin of neurodegeneration, is a subject of debate. While some studies have localized the area of greatest degenerative change to the anterior fusiform or inferior temporal gyrus (Seeley *et al.*, 2009), others consider the temporal pole (Mummery *et al.*, 2000; Galton *et al.*, 2001; Davies *et al.*, 2009; Rohrer *et al.*, 2009), entorhinal cortex (Chan *et al.*, 2001), or perirhinal cortex (La Joie *et al.*, 2014) to be the most prominent region of neurodegeneration. Although these discrepancies might be the result of biological variability between samples, they may also arise from differences in the neuroimaging analysis techniques used, which include voxel-based (VBM; Mummery *et al.*, 2000; Gorno-Tempini *et al.*, 2004; Seeley *et al.*, 2009), manual region of interest tracing (Chan *et al.*, 2001; Galton *et al.*, 2001), cortical thickness analyses (Rohrer *et al.*, 2009), or voxel-based analysis of hypometabolism obtained using ^{18}Fluorodeoxyglucose (FDG-PET; La Joie *et al.*, 2014). No studies have attempted to assess the reliability of effects across multiple samples of patients with svPPA.

Beyond the anterior temporal cortex, a distributed set of brain regions undergoes neurodegeneration in svPPA. Support for the hypothesis that neurodegenerative diseases selectively target large-scale networks identifiable in the healthy brain (Mesulam, 2000; Buckner *et al.*, 2005; Seeley *et al.*, 2009) has come from studies demonstrating considerable overlap between the topography of atrophy in patients with neurodegenerative diseases and that of distributed neural networks identified in healthy subjects using resting state functional connectivity (Seeley *et al.*, 2009; Zhou *et al.*, 2012; La Joie *et al.*, 2014) or diffusion-weighted imaging (Raj *et al.*, 2012). With regard to networks relevant to svPPA, a recent study from our lab has identified the anterior temporal cortex as a point of convergence for four large-scale sensory, association, and paralimbic functional-anatomic brain networks. In svPPA, physiological abnormalities appear to extend all the way back to posterior primary visual and auditory sensory cortex (Guo *et al.*, 2013). These previous findings demonstrating the functional heterogeneity (Ding *et al.*, 2009; Pascual *et al.*, 2015) and distributed connectivity (Guo *et al.*, 2013) of the anterior temporal lobes underscore the importance of identifying the precise focal point of neurodegeneration in svPPA and the intrinsic connectivity of this region in the healthy brain. Knowledge of the putative site of origin of neurodegeneration in svPPA and its connectivity will further elucidate whether principles governing the organization of large-scale functional networks provide insights into the distributed atrophy patterns in svPPA.

In the present study we used cortical thickness analysis and surface-based inter-subject registration to precisely localize the point of maximal atrophy in svPPA using an unbiased whole-cortex approach. We expanded upon previous analyses of focal atrophy in svPPA by investigating the reliability of the localization of this focal atrophy point in two independent samples, examining both the maximal atrophy point for each of the two sample groups versus older healthy controls, as well as the overlap of the maximal atrophy point between individual subjects. We then used resting state functional connectivity MRI (rs-fcMRI) in healthy young adults to assess the intrinsic network connectivity of this region. We predicted that the point of maximal atrophy in svPPA (i) would be replicable across independent patient samples and across a series of individual patients; and (ii) would be interconnected with an intrinsic neural network in healthy adults whose topography mimics the topography of distributed atrophy in svPPA. The latter finding would support previous observations that the topography of regional atrophy in patients with neurodegenerative diseases respects the topography of large-scale networks in the healthy brain and improve our understanding of disease onset and progression in svPPA. We further predicted, as a novel test of the network neurodegeneration hypothesis, that the strength of connectivity of every region within the large-scale healthy network to the putative onset site would predict the magnitude of that

region's atrophy in svPPA. Such a finding would extend previous tests of the network neurodegeneration hypothesis (Zhou *et al.*, 2012) by further supporting the notion that progressive neurodegeneration in svPPA follows the topography of connectional architecture and prioritizes the strongest connections from the site of origin.

Materials and methods

Participants

Control groups

The sample for the cortical thickness analysis included 30 older adults (15 females, age mean = 65.06, SD = 6.18, range = 52–80 years) who underwent detailed clinical and cognitive assessments and were determined to be cognitively normal. The sample for the rs-fcMRI analysis included 89 young adults [45 females, age mean = 22.4, standard deviation (SD) = 3.34, range = 18–33 years]. Our choice of a young adult healthy control group for the rs-fcMRI analysis was motivated by the fact that the topography of large-scale intrinsic networks is largely preserved across age, and recent work (Grothe *et al.*, 2016) has shown that intrinsic networks identified in healthy young adults recapitulate the patterns of pathology, hypometabolism, and atrophy in neurodegenerative disease. All control participants were right-handed native English speakers with normal or corrected-to-normal vision, and no history of neurological or psychiatric disorders. All participants gave written informed consent in accordance with the institutional review board of the Massachusetts General Hospital and Partners Healthcare System Human Research Committee.

Patients

Two independent samples of patients with svPPA were included in this study. The first patient sample was recruited from an ongoing longitudinal study being conducted in the Massachusetts General Hospital (MGH) Frontotemporal Disorders Unit. The MGH sample included 16 patients with svPPA (nine females, age mean = 64.01, SD = 7.37, range = 53–78 years). The second patient sample was recruited from the Memory and Aging Center at the University of California San Francisco (UCSF). The UCSF sample included 28 svPPA patients (18 females, age mean = 63.84, SD = 8.1, range = 49–80 years). All participants in both samples gave written informed consent, and the institutional review boards at MGH/Partners and UCSF approved the relevant studies. All patients with svPPA in both samples (Tables 1 and 2) were evaluated using a structured clinical assessment performed by a behavioural neurologist and speech pathologist, as previously described (Sapolsky *et al.*, 2010; Wilson *et al.*, 2014).

Patients were diagnosed with semantic variant PPA based on recent guidelines (Gorno-Tempini *et al.*, 2011). A diagnosis of PPA required progressive deterioration of speech and/or language functions, and that deficits be largely restricted to speech and/or language for at least the first 2 years of the illness (Mesulam, 2003). All patients included here had semantic language impairments and cortical atrophy that was most prominent in the left anterior temporal lobes upon first assessment. Visual inspection of a clinical MRI ruled out other causes of focal brain damage and in all cases provided imaging support for the diagnosis (anterior temporal atrophy).

Image acquisition

Massachusetts General Hospital sample

Imaging data for the MGH patient sample were collected on a 3 T Magnetom Tim Trio system at MGH (Siemens), using a 12-channel phased-array head coil. Structural data for the MGH patient sample were acquired using a standard T_1-weighted 3D MPRAGE sequence that varied slightly across patients. Nine patients were scanned using the following parameters: repetition time/echo time/flip angle = 2.53 s/3.48 ms/12°, resolution = 1.0 m isotropic. Three patients were scanned using the following parameters: repetition time/echo time/flip angle = 2.53 s/1.61 ms/12°, resolution = 1.0 m isotropic. Three patients were scanned using the following parameters: repetition time/echo time/flip angle = 2.30 s/2.98 ms/16°, resolution = 1.0 m isotropic. One patient was scanned using the following parameters: repetition time/echo time/flip angle = 2.53 s/6.8 ms/16°, resolution = 1.0 m isotropic.

University of California San Francisco sample

Structural data for the UCSF patient sample were acquired on a 1.5 T Magnetom VISION system at UCSF (Siemens), using a standard quadrature head coil. For each patient a T_1-weighted image of the entire brain was obtained using a MPRAGE sequence (repetition time/echo time/flip angle = 10 s/4 ms/15°, 1.0 × 1.0 mm^2 in-plane resolution, 1.5 mm slab thickness).

Healthy controls

Imaging data for both healthy adult samples were collected on a 3 T Magnetom Tim Trio system at MGH (Siemens), using a 12-channel phased-array head coil. Structural data for the older control sample ($n = 30$) were acquired using one of two T_1-weighted 3D MPRAGE sequences (repetition time/echo time/flip angle = 2.30 s/2.98 ms/16°, or repetition time/echo time/flip angle = 2.53 s/3.45 ms/12°, resolution = 1.0 mm isotropic for both sequences). Structural data for the young control sample ($n = 89$) were also acquired using a T_1-weighted 3D MPRAGE sequence (repetition time/echo time/flip angle = 2.2 s/1.54 ms/7° resolution = 1.2 mm isotropic). Functional MRI data for the young control sample were acquired for 6 mins during rest using a gradient-echo, echo-planar sequence with the following parameters: repetition time = 3000 ms; echo time = 30 ms; flip angle = 85°, 47 slices; voxel resolution: 3 mm isotropic. During the rs-fcMRI run participants were directed to keep their eyes open and to remain as still as possible.

Data processing and statistical analysis

Cortical thickness analyses

Cortical reconstructions of the T_1-weighted images were performed using the FreeSurfer analysis suite version 5.3.0 (https://surfer.nmr.mgh.harvard.edu/) using a procedure that

Table 1 Demographic and clinical data for the MGH svPPA patient sample

Case	Age	Age of onset	Gender	Education	CDR	MMSE	BNT (%)	CBS Naming (%)	CBS WPM (%)	PPT (%)	WAB SS	WAB Rep (%)
1	53	47	M	20	0.5	20	3%		27%	63%		84%
2	72	62	F	18	0.5	23	3		83		9	90
3	70	65	F	12	0.5	-			59	73	6	69
4	59	54	F	12	0.5	25		13	63	68	8	
5	79	74	M	18	0.5	19	33		91	81	10	96
6	58	55	M	16	1.0	28			50	50	8	
7	71	66	M	12	0.5	19		69	94		10	
8	61	57	M	14	0.5	24		20	53		10	
9	70	62	F	18	0.5	25	18	19	83		8	
10	63	61	F	16	0.5	6						
11	55	49	F	16	0.5	24	7		58	75		85
12	53	49	F	18	-	-	7		75			6
13	62	60	F	13	1.0	21			42	71		78
14	61	57	M	16	0.5	24	3		19	54		93
15	61	57	F	16	0.0	27	27					
16	62	58	M	20	0.0	28	57		94	100	10	98

Empty cells indicate missing data.

BNT = Boston Naming Task; CBS Naming = Cambridge Semantic Battery Naming Task; CBS WPM = Cambridge Semantic Battery Word Picture Matching Task; CDR = global score on the Clinical Dementia Rating Scale; MMSE = global score on the Mini-Mental Status Examination; PPT = Pyramids and Palm Trees; WAB Rep = Western Aphasia Battery Repetition Test; WAB SS = Western Aphasia Battery Spontaneous Speech (0 = severely impaired, 10 = normal).

has been previously described in detail (Dale *et al.*, 1999; Fischl *et al.*, 1999; Fischl and Dale, 2000; Rosas *et al.*, 2002; Salat *et al.*, 2004). All individual cortical reconstructions were manually inspected to check for accuracy blind to group affiliation, and any errors in the automatic segmentation of the grey/white matter boundary were manually corrected (Fischl *et al.*, 2001). Importantly, the scans of many patients with svPPA (MGH: 16/16, UCSF: 20/28) required substantial manual editing because the automated reconstruction did not correctly identify the grey–white junction due to the prominence of atrophy (Supplementary Fig. 1). Two independent investigators checked every coronal slice of the MGH svPPA patient sample after manual edits were made to ensure that the newly formed white matter and pial surfaces respected the topography of the underlying anatomy. The scans of the healthy controls did not require manual editing. This boundary was then used by the deformable surface algorithm to identify the pial surface (Fischl and Dale, 2000) for each subject. Cortical thickness was measured by calculating the distance between the white matter and pial surfaces at ~160 000 points (vertices) in each cerebral hemisphere. Each subject's reconstructed brain was then morphed and registered to an average spherical space that optimally aligned gyral and sulcal features, thus enabling the accurate matching of cortical locations among individuals across the entire cortical surface. Individual thickness measures were mapped into this new space. A Gaussian kernel of 10 mm full-width at half-maximum was applied to the subjects' cortical thickness maps before further analyses.

Cortical thickness group comparisons were performed using a 2-class general linear model (GLM) for the effect of clinical status, as implemented in FreeSurfer. Several group analyses were performed: one comparing each patient sample (MGH and UCSF) to the older healthy control group, one comparing the pooled (MGH and UCSF combined) svPPA patient sample to the older healthy control group, and one comparing each individual patient to the entire older healthy control group (Fig. 1).

Resting state functional connectivity MRI analyses

All rs-fcMRI data were first preprocessed using the following steps: removal of the first four functional volumes to allow for T_1-equilibration effects, slice timing correction (SPM2, Wellcome Department of Cognitive Neurology, London, UK), head motion correction using rigid-body transformation in three translations and three rotations (FMRIB, Oxford, UK), spatial normalization to standard (MNI-152) atlas space, resampling to 2 mm isotropic voxels, spatial smoothing with a 6 mm full-width at half-maximum Gaussian kernel, and low-pass temporal filtering to remove frequencies >0.08 Hz. Sources of spurious variance and their temporal derivatives were removed from the preprocessed data using linear regression. These sources of spurious variance included the six parameters derived from head-motion correction, the signal averaged over the whole brain, the average signal from a region located deep in white matter, and the average signal from ventricular CSF. A 4 mm spherical seed region (region of interest) was generated centred on the focal svPPA atrophy point identified in the cortical thickness analysis. A correlation map for this seed was generated by computing the Pearson's product moment correlation 'r' between every voxel in the brain and the average mean signal time course of the voxels within this sphere. Positive values in this map were then converted to *z*-scores using Fisher's r-to-z transformation for comparison with a pooled cortical atrophy map derived from both svPPA patient samples. In keeping with previous work (Pascual *et al.*, 2015) we chose a liberal threshold ($z > 0.04$) that has been frequently used in rs-fcMRI studies because it provides

Table 2 Demographic and clinical data for UCSF svPPA patient sample

Case	Age	Age of onset	Gender	Education	CDR	MMSE	BNT (%)	PPVT	WAB AWRT (%)	PPT (%)	WAB SS	WAB Rep (%)
1	56	53	M	12	0.5	23	13		100			
2	75	72	F	16	1	22	67			62	10	98
3	62	60	M	18	0.5	3			87			
4	61	57	M	18	0.5	28	27		100		9	82
5	71	68	F	16	0	28	33		38	94		
6	65	60	M	17	0.5	16	0	100	100		8	70
7	56	54	F	22	0	30	47			92	10	96
8	73	72	F	16	0	19	7					
9	68	66	F	19	0.5	23		6	50			
10	67	60	F	14	1	7	13		100	52		60
11	58	56	M	16	0.5	29	20		87	92	9	100
12	62	57	F	14	0.5	19	0		72	56	9	96
13	62	58	F	14	0.5	8	13		93	83	6	60
14	60	53	F	18	0.5	26	13	19	85	65	10	95
15	80	71	M	18	1	13		25	85	56	7	97
16	56	50	M	12	0.5	20	7	38	100	71	9	84
17	64	52	F	12	0.5	28	20	63	100	65	9	93
18	65	61	M	16	0.5	29	40	69	100	85	10	94
19	61	57	F	11	1	30	53	25	97			87
20	64	59	M	13	0.5	26	13	25	58	67	10	97
21	67	56	M	20	1	12	13	31	98		8	73
22	49	48	M	12	0.5	26	27	75	100	88	9	81
23	72	67	M	16	0.5	30	67	69	100	92	9	100
24	66	60	F	19	1	26	67	69	95	90	10	93
25	55	53	M	14	1	27	27	56	95		9	89
26	74	72	F		0.5	22	7	38		81	9	89
27	57	46	F	18	1	28	33			96		
28	61	57	M	18	1	15	7					

Empty cells denote missing data.

BNT = Boston Naming Task; CBS Naming = Cambridge Semantic Battery Naming Task; CBS WPM = Cambridge Semantic Battery Word Picture Matching Task; CDR = global score on the Clinical Dementia Rating Scale; MMSE = global score on the Mini-Mental Status Examination; PPT = Pyramids and Palm Trees; WAB Rep = Western Aphasia Battery Repetition Test; WAB SS = Western Aphasia Battery Spontaneous Speech (0 = severely impaired, 10 = normal).

results that are similar to the results obtained with independent component analysis (Van Dijk *et al.*, 2010). Non-parametric permutation testing (5000 permutations) was performed on the resulting *z*-score maps using FSL Randomise (Winkler *et al.*, 2014), correcting for multiple comparisons using the threshold-free cluster enhancement (TFCE) technique [statistical threshold was set at $P < 0.05$, family-wise error (FWE) corrected]. All rs-fcMRI results were projected to the pial surface for comparison with the results of the cortical thickness analyses.

Relating connectivity to atrophy

First, the entire cortex of the average spherical surface was microparcellated into 642 regions of interest of similar area (mean = 255.2 vertices, SD = 2.49 vertices) per hemisphere, without adhering to any anatomical boundaries. Only regions of interest that had at least 70% of their vertices within the atrophy mask (binarized at $P < 0.01$) for each sample and at least one vertex with a rs-fcMRI *z*-value > 0.04 were used in further analysis, resulting to a total of 209 regions of interest for the MGH sample and 275 for the UCSF sample. The mean cortical thickness for each region of interest (averaged across all vertices within the region of interest) was calculated for each patient sample using the appropriate sample-specific atrophy mask. Mean cortical thickness for all regions of interest in both patient sample atrophy masks was also calculated for the older healthy control group. The relative percentage of atrophy in each region of interest was then calculated for each patient sample separately using the following formula: [1 − (mean patient cortical thickness / mean older healthy control group cortical thickness)] × 100.

The average normalized (*z*) rs-fcMRI of each sample-specific region of interest with the focal atrophy point was also extracted from the young healthy control group rs-fcMRI map. The Pearson's product-moment correlation coefficient 'r' was then computed between the rs-fcMRI of each region of interest in young healthy control groups and cortical atrophy in each region of interest for each patient group. The region of interest containing the temporal pole seed for the rs-fcMRI map was excluded from both correlation analyses to avoid artificially inflating the estimated connectivity of this region. As an additional control we repeated both analyses using partial correlations controlling for the Euclidean distance (in MNI space) between the centre of each region of interest, and the centre of the temporal pole seed region.

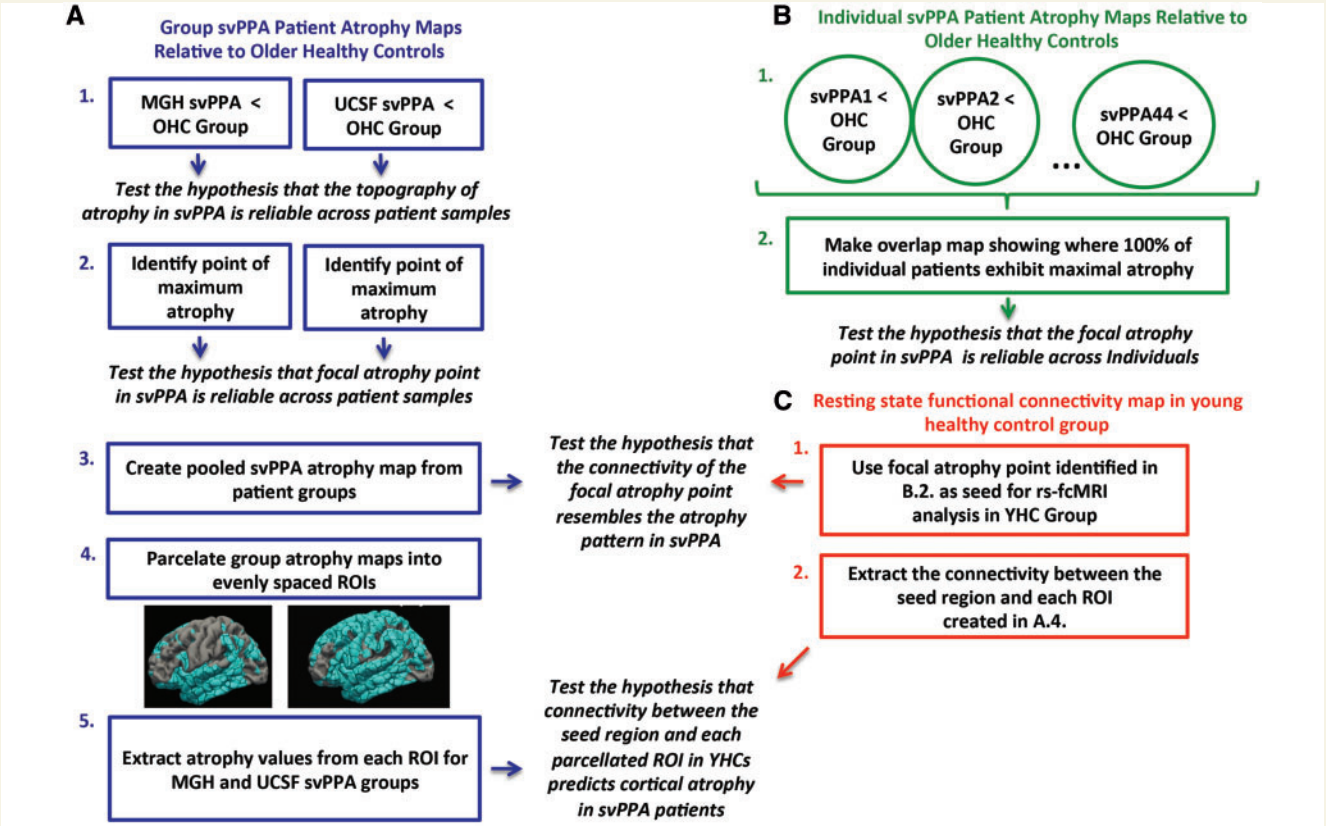

Figure 1 Schematic representation of study design. Three independent analysis streams were used to test hypotheses (displayed in italics) about the topography and point of focal atrophy in svPPA. The steps used in each analysis stream are numbered and enclosed by squares. Arrows point to the specific hypothesis tested in each analysis step. (**A**) Analyses performed on group maps of cortical atrophy in the MGH and UCSF svPPA samples. (**B**) Analyses performed on individual maps of cortical atrophy across both svPPA patient samples. (**C**) Analyses performed on rs-fcMRI map derived from a young healthy control (YHC) group. OHC = older healthy control group; ROI = region of interest.

Results

The focal point of cortical atrophy in svPPA is localized to the left temporal pole

Both svPPA patient samples demonstrated substantial cortical atrophy relative to healthy controls that was—while most prominent in the left anterior temporal cortex—distributed throughout portions of left medial and lateral temporal cortex, left anterior insula, left ventromedial prefrontal and orbitofrontal cortex, left anterior and posterior cingulate, and left inferior parietal lobule (Fig. 2A); the right anterior temporal cortex was also consistently atrophied, although generally to a much lesser degree than the left. Visual inspection of the maps revealed more widespread cortical atrophy in the UCSF patient sample (than in the MGH sample) that extended into the left and right superior frontal gyrus. This likely reflects the difference in sample size (28 versus 16) and resultant differences in statistical sensitivity between the two patient groups. To localize the most atrophied point in both patient samples, we imposed a threshold on each group map that included vertices with atrophy *P*-values in the top 98% (min 10^{-30} and 10^{-38} for the MGH and UCSF samples, respectively). This stringent thresholding localized a global maxima for each patient group that was located in area TG of the left temporal pole (Ding *et al.*, 2009; Pascual *et al.*, 2015) that was strikingly similar across both patient groups (MNI coordinates for the MGH sample: −42, 16, −30, UCSF sample: −42, 16, −30, Fig. 2B).

The focal point of cortical atrophy is highly reliable across individual patients

Individual patterns of cortical atrophy can vary substantially within patients of the same diagnosis, and do not necessarily mirror atrophy patterns identified at the group level. Thus, in the present study we assessed the similarity of atrophy patterns in single patients by computing the vertex-wise difference in cortical thickness of each of the 44 patients with svPPA against the group of older adult healthy controls. Each of the resulting single-subject maps was then binarized to include only the top 1% of *P*-values. These maps were then combined creating a heat-map displaying—for each vertex—the percentage of

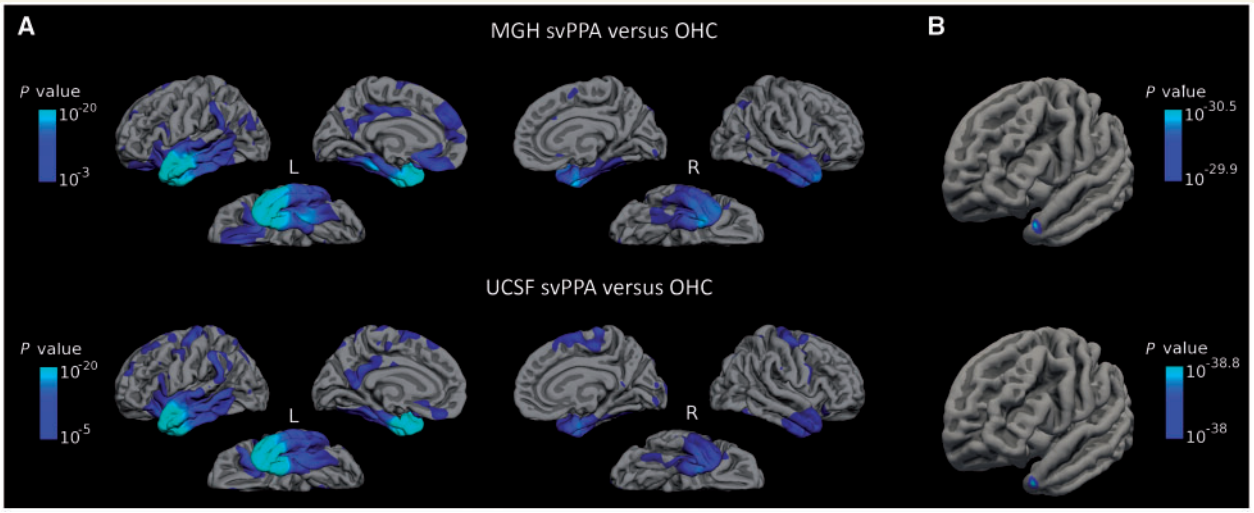

Figure 2 Cortical atrophy is localized in a highly consistent fashion in MGH and UCSF svPPA samples, and is most prominent in the temporal pole. (**A**) Relative to healthy controls, svPPA patients from the MGH sample (*top row*) and UCSF sample (*bottom row*) displayed an asymmetric pattern of cortical atrophy that was most prominent in the left anterior temporal cortex. Due to differences in the sample size of each patient group, different colour-scale values were used to allow optimal visualization of the localization of atrophy. (**B**) The maximal point of cortical atrophy in both patient groups was localized in the left temporal pole, consistent with area TG. OHC = older healthy control group.

patients with this region as their most atrophic point (Fig. 3A). Remarkably, the maximal atrophic point (top 1% of *P*-values) for 100% of the patients with svPPA was located in a small region of the left lateral temporal pole (MNI coordinates: −43, 15, −29) and in a small region of the left medial temporal pole (MNI coordinates: −27, 8, −36). Other regions, such as the rostral fusiform gyrus or the rostral tip of the temporal pole were affected in at least 75% of patients. The region identified in the lateral temporal pole that was affected maximally in 100% of patients overlaps entirely with the focal atrophy point identified in our previous analysis of focal atrophy in each patient group (Fig. 2B). Cortical thickness in this region did not differ significantly between the two patient populations ($P = 0.27$, Fig. 3B), but was much lower in patients relative to controls ($P = 1.01 \times 10^{-42}$). Notably, average thickness in the patient group was 1.49 mm, while in controls it was 3.7 mm, a loss of $>50\%$ of the cortical mantle in patients. An additional analysis of mean cortical thickness in a control region in the inferior frontal sulcus, which was selected because it falls outside of the typical pattern of cortical atrophy in patients with svPPA (reviewed in Diehl-Schmid *et al.*, 2014), revealed no difference between patients and controls ($P = 0.25$).

The distributed cortical connectivity of the healthy temporal pole resembles the distributed atrophy pattern in svPPA

Investigating the distributed cortical connectivity of the tip of the temporal pole—the focal point of atrophy in svPPA—revealed a network of brain regions in healthy young adults (threshold at $P < 0.05$, FWE corrected) that enveloped 64.88% of the atrophy map identified in our cortical thickness analysis of the combined svPPA patient group (Fig. 4C). This connectivity pattern was present in portions of the bilateral anterior temporal cortices (parahippocampal gyrus, fusiform gyrus, inferior and middle temporal gyrus); frontal cortices (orbitofrontal cortex, medial, ventrolateral, and dorsolateral prefrontal cortex); inferior parietal lobule (angular gyrus and supramarginal gyrus); precuneus and posterior cingulate cortex. The area of focal atrophy also displayed functional connectivity with several subcortical brain regions, including the bilateral amygdala and hippocampi (data not shown). This network of brain regions is strikingly similar to a functional-anatomic network that our lab recently dubbed the default-semantic network (Pascual *et al.*, 2015), which is interconnected with areas TG and TE of the temporal pole, and encompasses much of the default mode network (Buckner *et al.*, 2008) and several regions implicated in semantic cognition (Binder *et al.*, 2009). The earliest available MRI scan was used for the cortical thickness analysis of each svPPA patient included here. Thus, one possibility is that brain regions that are functionally connected with the temporal pole focal atrophy point, but not yet damaged in this sample, may be regions vulnerable to atrophy at later stages of the disease.

The strength of healthy connectivity within the large-scale intrinsic temporal pole network predicts the magnitude of cortical atrophy in svPPA

We computed the Pearson's product-moment correlation coefficient 'r' between (i) the per cent of cortical atrophy

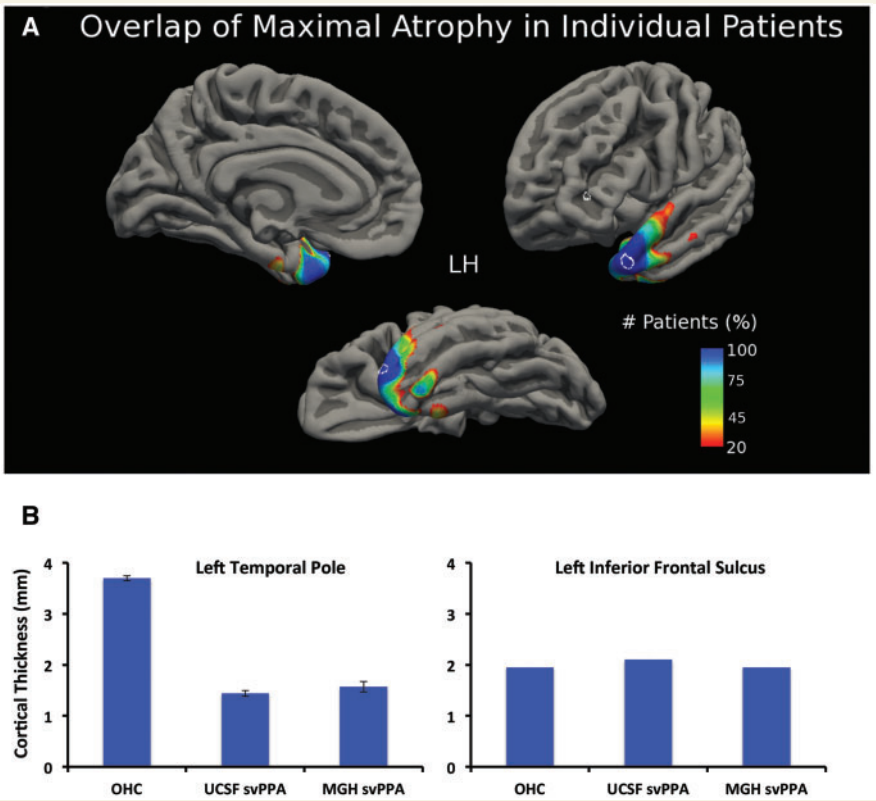

Figure 3 Cortical atrophy in each individual svPPA patients overlaps with the same area of the left temporal pole identified in the group analysis. (**A**) A heat map based on individual patients atrophy maps revealed that 100% of patients had their maximal atrophy point (top 1% of cortical atrophy) in the same region of the left temporal pole, just lateral to the tip (circled; MNI coordinates: $x = -42$, $y = 17$, $z = -31$) and a small area at the medial region (MNI coordinates: $x = -27$, $y = 7$, $z = -36$). (**B**) Relative to controls, cortical thickness was substantially lower in patients in this focal atrophic point of the left temporal pole (thickness of this region in patients is less than half of that of controls). In contrast, a control region placed in the left inferior frontal sulcus did not differ in thickness between patients and controls (also circled in **A**). OHC = older healthy control group.

in each microparcellated region of interest for each of the two svPPA patient samples; and (ii) the average normalized rs-fcMRI value (z) of each region of interest with the temporal pole seed region in young healthy control groups (Fig. 5A). In both patient samples a moderate-to-strong correlation was observed between the magnitude of cortical atrophy in a region of interest, and that region of interest's rs-fcMRI with the temporal pole seed region in young healthy control groups (MGH: $r = 0.4$, $P < 0.001$; UCSF: $r = 0.5$, $P < 0.001$). We additionally computed Pearson's 'r' between (i) the per cent of cortical atrophy in each region of interest for each svPPA sample; and (ii) the Euclidean distance (in MNI space) between each region of interest and the temporal pole seed region. In both patient samples a moderate-to-strong negative correlation was observed between the magnitude of cortical atrophy in a region of interest, and that region of interest's Euclidean distance to the temporal pole seed (MGH: $r = -0.47$, $P < 0.001$; UCSF: $r = -0.39$, $P < 0.001$). The absolute values of the correlation coefficients between the magnitude of atrophy in each region of interest and that region of interest's Euclidean distance to the seed, or rs-fcMRI with the seed, did not differ significantly in either patient group (MGH: $z = 0.85$, $P = 0.39$; UCSF: $z = 1.68$, $P = 0.09$). Furthermore, in each patient sample there was no significant correlation between the Euclidean distance of each region of interest to the temporal pole seed, and the rs-fcMRI of each region of interest with the temporal pole seed in young healthy control groups, suggesting that each measure might be contributing unique variance to the magnitude of atrophy in each region of interest in svPPA (MGH: $r = -0.02$, $P = 0.74$; UCSF: $r = -0.11$, $P = 0.06$).

We conducted a series of partial correlation analyses to assess the unique contributions of temporopolar rs-fcMRI and Euclidean distance to the magnitude of atrophy in each region of interest. In both patient samples the effect of rs-fcMRI remained significant after controlling for the Euclidean distance (in MNI space) between each region of interest and the temporal pole seed (MGH: $r = 0.47$, $P < 0.001$; UCSF: $r = 0.5$, $P < 0.001$). Additionally, in both samples the effect of Euclidean distance remained significant after controlling for rs-fcMRI with the temporal pole seed (MGH: $r = -0.52$, $P < 0.001$; UCSF: $r = -0.38$, $P < 0.001$). We interpret these results to indicate that, if

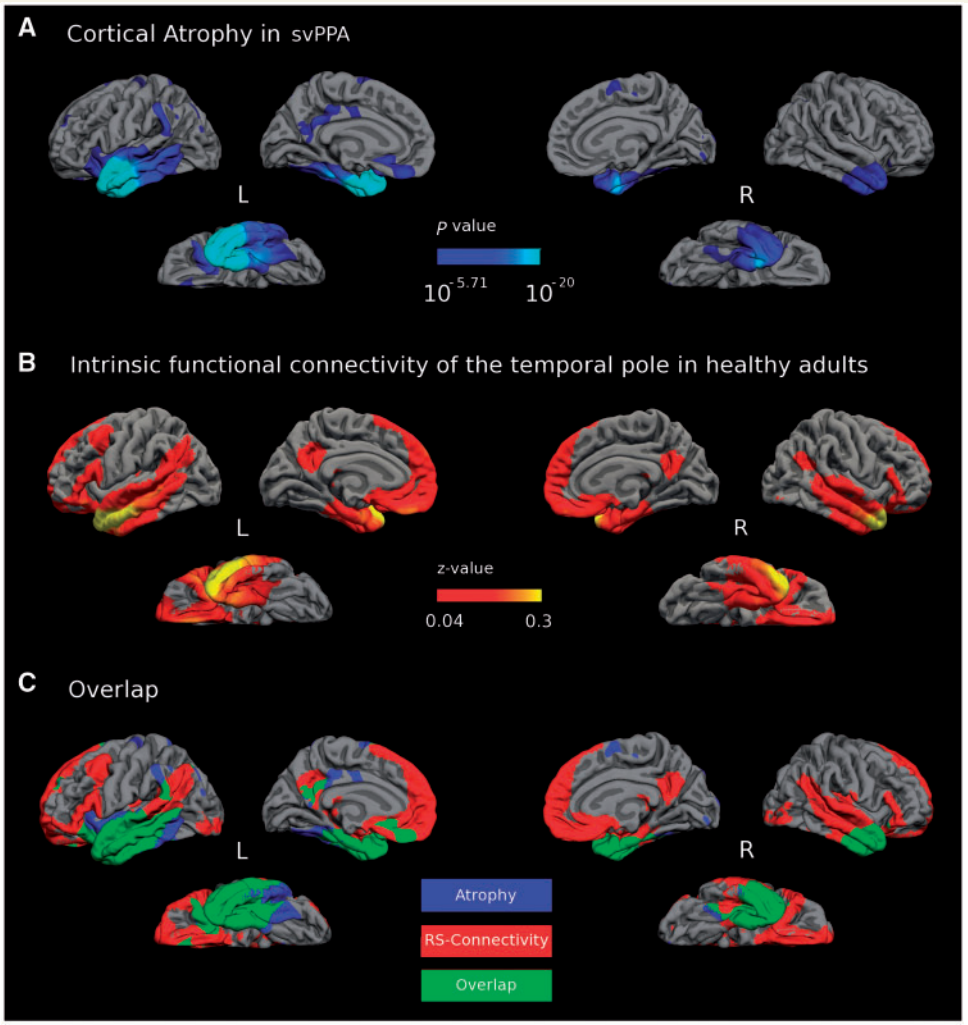

Figure 4 Convergence of healthy large-scale network connectivity and atrophy in svPPA. (**A**) Pooled cortical atrophy map, including patients from both the MGH and UCSF samples ($n = 44$, FDR corrected $P < 0.0001$). (**B**) The temporal pole area of greatest atrophy in svPPA (Fig. 1B) was used as a seed to generate a resting-state (RS) functional connectivity map of a large-scale intrinsic connectivity network in healthy adults (FWE corrected $P < 0.05$). (**C**) The topography of these two maps shows substantial overlap (green) between the large-scale intrinsic temporal pole network in healthy individuals (binarized at $z > 0.04$, only including vertices that survived an FWE correction for multiple comparisons $P < 0.05$) (red) and cortical atrophy in the pooled patient sample (FDR corrected $P < 0.0001$, blue).

atrophy in svPPA is assumed to progress linearly, it progresses in a manner dictated by both the strength of connections with the site of origin and physical distance from the site of origin.

Discussion

Although the most prominent neurodegeneration in svPPA is unquestionably within the anterior temporal cortex, the precise localization of its epicentre has been a subject of debate. Using cortical thickness analysis and cortical surface-based registration in two independent samples of patients with svPPA, we found that the point of maximal cortical atrophy—likely the initial neurodegenerative lesion—is localized reliably in the left temporal pole, slightly dorsolateral to the tip. We further investigated the reliability of focal atrophy across individual patients and found that 100% of individuals in both svPPA samples had one of their maximally atrophic points in the same temporopolar region. Beyond the anterior temporal cortex, patients with svPPA exhibit less prominent neurodegeneration in distributed cortical and subcortical regions (Mummery *et al.*, 2000; Rosen *et al.*, 2002; Gorno-Tempini *et al.*, 2004; Brambati *et al.*, 2009; Rohrer *et al.*, 2009). As predicted, the focal atrophy point identified in our cortical thickness analysis was interconnected with a network of brain regions in healthy adults that closely resembled the distributed cortical atrophy pattern of svPPA patients, replicating previous findings (Seeley *et al.*, 2009). Furthermore, the magnitude of cortical atrophy within a given brain region in both samples of svPPA patients was predicted

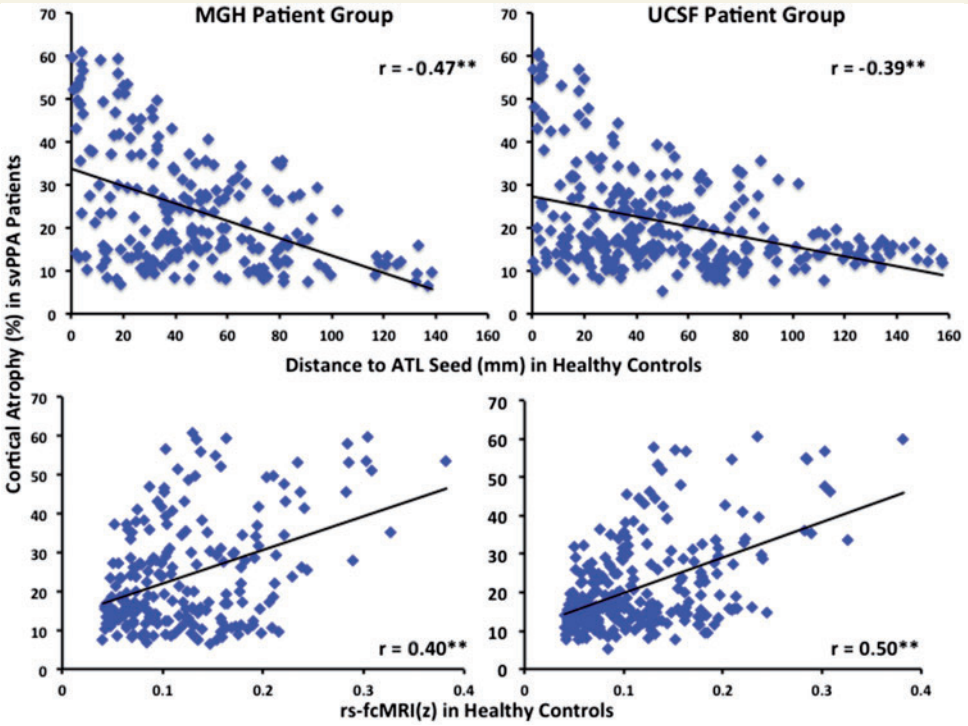

Figure 5 Strength of connectivity of distributed cortical regions with the temporal pole in healthy adults predicts magnitude of atrophy within distributed cortical regions in svPPA patients. Within each region of interest the Euclidean distance to the temporal pole (*top*), and the strength of its functional connectivity with the temporal pole in young healthy adults (*bottom*) predicted the magnitude of cortical atrophy in both svPPA patient cohorts (**$P < 0.001$). The region of interest containing the temporal pole seed for the rs-fcMRI map was excluded from all correlation analyses.

by that region's connectivity strength and Euclidean distance to the temporal pole in healthy adults. This provides additional support for the hypothesis that progressive neurodegeneration in svPPA follows connectional pathways within a large-scale neural network that is connected to the temporal pole.

Reliability of focal atrophy in svPPA

Prior work aiming to localize the most prominent degenerative change in svPPA has produced a variety of results, including the anterior fusiform or inferior temporal gyrus (Seeley *et al.*, 2009), temporal pole (Mummery *et al.*, 2000; Galton *et al.*, 2001; Davies *et al.*, 2009; Rohrer *et al.*, 2009), entorhinal cortex (Chan *et al.*, 2001), and perirhinal cortex (La Joie *et al.*, 2014). This variability likely reflects differences in the neuroimaging analysis technique used and biological variability between patient samples. Here, using cortical thickness analysis we identified a point of focal atrophy that was consistent across 44 individual patients and two neuroimaging centres. Previous analyses of neurodegeneration in svPPA that were conducted in volume space, using either VBM or PET, may have lacked the spatial precision necessary to identify a reliable point of maximal abnormality (Iaccarino *et al.*, 2015). Even when conducted at high spatial resolutions, single volumetric units (voxels) can contain segments of grey and white matter depending on thresholding and image acquisition parameters. Furthermore, single voxels may cut across gyral/sulcal boundaries limiting the degree to which individual subjects can be aligned according to cortical anatomy. The use of cortical thickness analyses enabled us to detect the most prominent area of cortical atrophy with sub-millimetre precision without interference from cortical folding. Furthermore, we used surface-based inter-subject registration, which optimally aligns gyral and sulcal features across individual subjects and enables the precise matching of morphologically homologous cortical locations while reducing geometric distortion (Fischl *et al.*, 1999; Fischl and Dale, 2000). The pathologically thin temporopolar cortex in svPPA—less than half its typical thickness—can readily be seen in post-mortem tissue and likely reflects substantial cell loss in cortical grey matter. The reliability of the localization of this effect, our experience that many patients exhibit prominent atrophy at initial clinical presentation, and the fact that the temporal pole does not usually undergo atrophy in normal ageing (Bakkour *et al.*, 2013) offer the opportunity to consider this measure as a biomarker that could be used in the in-depth evaluation of patients presenting with mild symptoms of memory, language, or obvious semantic impairment.

An important caveat of the current research is that it is currently unclear whether regions with greater cortical atrophy are necessarily those that begin deteriorating first. Longitudinal (Rogalski *et al.*, 2011, 2014) and cross-sectional (Rohrer *et al.*, 2009) studies have shown that atrophy is apparent in the left temporal pole early in svPPA; however, some of these patients exhibit fairly widespread atrophy by the time they reach clinical attention and receive a diagnosis. In the present sample, 10 patients received an MRI within 2 years of symptom onset (Supplementary Fig. 2). Individual atrophy maps for each of these patients revealed left temporopolar atrophy that was most prominent in the focal atrophy region identified with our larger sample. Furthermore, the magnitude of cortical thinning across the cortical mantle outside the anterior temporal lobe was predicted by disease duration to a much greater extent than in the temporal pole region of interest (Supplementary Fig. 3) supporting our speculation that the atrophic process may have completed in this region by the time these patients reach clinical attention. However, identifying a true origin of progressive atrophy in any neurodegenerative disease will necessitate the identification of patients even earlier, before atrophy has begun to spread throughout the cortex. At present, it is not clear how to identify svPPA patients earlier, since genetic or environmental risk factors are not known.

Functional implications of focal temporopolar atrophy in svPPA

Patients with svPPA usually exhibit impaired semantic memory across all modalities and object categories (Bozeat *et al.*, 2000; Hodges *et al.*, 2000; Lambon Ralph *et al.*, 2007; Luzzi *et al.*, 2007; Goll *et al.*, 2010; Piwnica Worms *et al.*, 2010), although initially have preserved performance for concepts with rich auditory or motor characteristics (Hoffman *et al.*, 2012). Previous work has associated diffuse atrophy in the left anterior temporal lobe with semantic processing deficits in semantic dementia (Mummery *et al.*, 2000). More recently, it has been shown that atrophy in a region of interest in the left temporal pole predicts semantic impairment in primary progressive aphasia (Sapolsky *et al.*, 2010). However, when a whole-brain regression is used, semantic memory impairments in patients with semantic dementia are best predicted by focal hypometabolism in the bilateral anterior fusiform gyrus (also known as perirhinal cortex) (Mion *et al.*, 2010). Thus, one possibility is that atrophy begins in the temporal pole but that semantic deficits manifest when the damage encroaches on a semantic hub in the anterior fusiform/perirhinal cortex (Mion *et al.*, 2010).

The selectivity of the cognitive impairments and cortical atrophy in svPPA are often cited in support of hub models of semantic memory. According to this account, modality-specific sensory information is integrated into multi-modal semantic representations in the rostral temporal poles (Patterson *et al.*, 2007; Lambon Ralph *et al.*, 2010; Baron and Osherson, 2011; Rice *et al.*, 2015*a*). It should be noted that this view is contentious, with other researchers arguing that there is no centralized semantic hub, and instead that semantic memory is subserved by a distributed network of sensory and motor brain regions (Martin, 2007; Binder *et al.*, 2009). Regardless, a large body of functional neuroimaging work has implicated the temporal poles in semantic processing (Damasio *et al.*, 2004; Patterson *et al.*, 2007; Visser *et al.*, 2010). Several laterality differences have been observed, with the left and right temporal poles being relatively more involved in tasks using stimuli that are verbal versus non-verbal (Damasio *et al.*, 2004; Butler *et al.*, 2009; Mion *et al.*, 2010; Gainotti, 2012, 2015; Rice *et al.*, 2015*a*, *b*) or non-social versus social (Olson *et al.*, 2007; Simmons and Martin, 2009; Wong and Gallate, 2012; Olson *et al.*, 2013). These specializations are graded (Rice *et al.*, 2015*a*, *b*), and may be driven in part by the differential connectivity of the left and right temporal poles with the extended language network in the left hemisphere, and with the extended face-processing network in the right hemisphere (Pyles *et al.*, 2013; Hurley *et al.*, 2015). Early atrophy of the left temporal pole in svPPA appears sufficient to produce semantic impairments for verbal stimuli (Mesulam *et al.*, 2013). The spread of atrophy to the right temporal pole and other nodes within this network likely contribute to the behavioural and social symptoms that are often observed as svPPA progresses (Mummery *et al.*, 2000; Rosen *et al.*, 2002; Seeley *et al.*, 2005; Chan *et al.*, 2009; Rohrer and Warren, 2010; Irish *et al.*, 2014).

Intrinsic network architecture and neurodegeneration in svPPA

Our results suggest that neurodegeneration in svPPA may originate in the left temporal pole and then preferentially targets brain regions with the strongest connections to the temporal pole. The hub architecture of the temporal pole may render it more vulnerable to initial neurodegeneration due to its high network centrality, which is hypothesized to facilitate activity-dependent 'wear and tear' (Buckner *et al.*, 2009). Consistent with this hypothesis, a previous study showed that cortical areas with greater network flow were more likely to constitute neurodegenerative disease-critical epicentres (Zhou *et al.*, 2012). The same study revealed that functional path distance to syndrome-specific epicentres predicted distributed cortical atrophy in multiple neurodegenerative disorders. These results are consistent with our finding that the strength of connectivity—in addition to physical distance—between the temporal pole and distributed cortical regions in healthy adults predicted the magnitude of cortical atrophy in patients with svPPA, supporting the concept that the spread of neurodegenerative pathology is guided in part by the connectivity of the point of origin.

In addition to the default-semantic network, area TG in the rostral temporal pole is heavily interconnected with the rest of the anterior temporal lobes (Pascual *et al.*, 2015). The connectivity of this region with other anterior temporal lobe regions may facilitate the spread of neurodegeneration across independent intrinsic networks and account for the cortical atrophy observed in both svPPA patient samples outside of the default-semantic network. Thus, it is possible that the atrophy observed in both patient samples in the insula and mid-cingulate may be partially attributable to the connectivity of these regions with area TA, which is located posterior and adjacent to area TG, is intrinsically connected to TG, and is interconnected with a network of brain regions important for auditory, somatosensory, and affective processing. This account is speculative, and further work using more refined neural network measures, such as graph theory (Bullmore and Sporns, 2009) or stepwise-connectivity (Sepulcre *et al.*, 2012), is necessary to advance our understanding of how cortical atrophy may progress within and across intrinsic neural networks.

Relating functional connectivity to white-matter pathways

Converging evidence has suggested that several neurodegenerative diseases may progress along white matter fibre tracts connecting large-scale networks (Englund *et al.*, 1988; Villain *et al.*, 2008; Kuczynski *et al.*, 2010). Supporting this hypothesis, laboratory evidence has shown that disease proteins can travel through local and long-range pathways via transynaptic spread (Frost *et al.*, 2009; Palop and Mucke, 2010; Sanders *et al.*, 2014). Although the relationship between the strength of functional connectivity and underlying white matter integrity is still being examined (Honey *et al.*, 2009; Van Den Heuvel *et al.*, 2009; Hermundstad *et al.*, 2013), the results of our rs-fcMRI analysis are broadly consistent with previously reported patterns of white matter degeneration in svPPA (Acosta-Cabronero *et al.*, 2011; Agosta *et al.*, 2012; Iaccarino *et al.*, 2015). In patients with svPPA, degeneration has been observed in white matter fibres projecting from the rostral temporal lobes into the arcuate, uncinate, and inferior longitudinal fasciculi (Agosta *et al.*, 2010, 2012, 2013*a*; Acosta-Cabronero *et al.*, 2011). Based on this previous work, and the results reported here, we speculate that selective atrophy in svPPA may originate in the left temporal pole and then proceed posteriorly to envelop the lateral temporal cortices and angular gyrus via the arcuate fasciculus, the orbitofrontal cortices via the uncinate fasciculus, and ventral temporal cortices via the inferior longitudinal fasciculus. Importantly, the dorsal part of temporal pole has been demonstrated to be interconnected with the angular and supramarginal gyri of the inferior parietal lobule via the middle longitudinal fascicle (Makris *et al.*, 2009, 2013*a*, *b*). This long association connection between the superior temporal pole and parietal regions may play an important role in word and sentence comprehension, as has recently been suggested by Mesulam *et al.* (2015).

Although atrophy in svPPA is more prominent in the left hemisphere, substantial atrophy also occurs in the right temporal pole (Rohrer *et al.*, 2009; Rogalski *et al.*, 2011; Brambati *et al.*, 2015). The right and left temporal poles have strong intrinsic functional connectivity and are structurally connected via the anterior commissure (Makris *et al.*, 1999; Catani *et al.*, 2002; Catani and Thiebaut de Schotten, 2008). Whether the anterior commissure is a conduit for the spread of pathogenic protein forms between the left and right temporal poles in svPPA remains an open question. To date, no studies have reported altered microstructural changes in the anterior commissure in svPPA patients, possibly due to the small size of this fibre bundle, which in part makes it difficult to delineate from other pathways that converge in the temporal poles (Patel *et al.*, 2010).

Limitations and future directions

There is variability in the cortical atrophy exhibited by patients with svPPA, with some patients having more involvement of lateral language or ventral visual semantic circuits and others having more involvement of medial paralimbic/affective networks. Additionally, some patients with semantic dementia (~30%) present initially with greater atrophy in the right anterior temporal lobe, and these patients often have greater social-emotional deficits along with prosopagnosia (Chan *et al.*, 2009; Hodges *et al.*, 2010; Irish *et al.*, 2013). Patient-specific neurodevelopmental factors likely contribute to the selective vulnerability of neural regions and networks to progressive degeneration (Rogalski *et al.*, 2008; Spreng *et al.*, 2010; Miller *et al.*, 2013), and may account for some of the variability observed in the atrophy patterns of patients with svPPA. In our patient sample, selective atrophy in the left temporal pole was remarkably consistent across individuals but much more variable in other brain regions. Additional work with larger sample sizes could help elucidate the patient-specific factors that drive the distribution of neuronal loss in svPPA.

Here we used the focal atrophy point in svPPA to investigate the functional connectivity of this region in a large group of young healthy adults. This same approach has been used in several previous studies (Seeley *et al.*, 2009; Zhou *et al.*, 2012; La Joie *et al.*, 2014) and has proven useful for explicating intrinsic neural networks that are robustly expressed in the population. However, there is some variability in neural network topology across individuals (Mueller *et al.*, 2013), and intrinsic neural networks may selectively reorganize in patients with neurodegenerative diseases (Xie and He, 2011; Agosta *et al.*, 2013*b*, 2014). An interesting avenue for future research will be to investigate the degree to which individual differences in the connectivity of the temporal poles (or other disease-related

focal atrophy points) predict the progressive spread of neurodegeneration within a single patient. The results reported here suggest a close correspondence between functional connectivity and progressive atrophy, and we expect an even closer correspondence will be observed when individual differences in connectivity are taken into account.

Funding

This work was supported by the following National Institutes of Health Grants: R21 NS077059, R01 NS050915, P01 AG005134. This research was carried out in whole or in part at the Athinoula A. Martinos Center for Biomedical Imaging at the Massachusetts General Hospital, using resources provided by the Center for Functional Neuroimaging Technologies, P41EB015896, a P41 Biotechnology Resource Grant supported by the National Institute of Biomedical Imaging and Bioengineering (NIBIB), National Institutes of Health. This work also involved the use of instrumentation supported by the NIH Shared Instrumentation Grant Program and/or High-End Instrumentation Grant Program; specifically, grant number(s) S10RR023401, S10RR023043, S10RR021110. The content is solely the responsibility of the authors and does not necessarily represent the official views of the National Institute of Health.

Supplementary material

Supplementary material is available at *Brain* online.

References

Acosta-Cabronero J, Patterson K, Fryer TD, Hodges JR, Pengas G, Williams GB, et al. Atrophy, hypometabolism and white matter abnormalities in semantic dementia tell a coherent story. Brain 2011; 134 (Pt 7): 2025–35.

Adlam AL, Patterson K, Rogers TT, Nestor PJ, Salmond CH, Acosta-Cabronero J, et al. Semantic dementia and fluent primary progressive aphasia: two sides of the same coin?. Brain 2006; 129 (Pt 11): 3066–80.

Agosta F, Galantucci S, Canu E, Cappa SF, Magnani G, Franceschi M, et al. Disruption of structural connectivity along the dorsal and ventral language pathways in patients with nonfluent and semantic variant primary progressive aphasia: a DT MRI study and a literature review. Brain Lang 2013a; 127: 157–66.

Agosta F, Galantucci S, Valsasina P, Canu E, Meani A, Marcone A, et al. Disrupted brain connectome in semantic variant of primary progressive aphasia. Neurobiol Aging 2014; 35: 2646–55.

Agosta F, Henry RG, Migliaccio R, Neuhaus J, Miller BL, Dronkers NF, et al. Language networks in semantic dementia. Brain 2010; 133 (Pt 1): 286–99.

Agosta F, Sala S, Valsasina P, Meani A, Canu E, Magnani G, et al. Brain network connectivity assessed using graph theory in frontotemporal dementia. Neurology 2013b; 81: 134–43.

Agosta F, Scola E, Canu E, Marcone A, Magnani G, Sarro L, et al. White matter damage in frontotemporal lobar degeneration spectrum. Cereb Cortex 2012; 22: 2705–14.

Bakkour A, Morris JC, Wolk DA, Dickerson BC. The effects of aging and Alzheimer's disease on cerebral cortical anatomy: specificity and differential relationships with cognition. Neuroimage 2013; 76: 332–44.

Baron SG, Osherson D. Evidence for conceptual combination in the left anterior temporal lobe. Neuroimage 2011; 55: 1847–52.

Binder JR, Desai RH, Graves WW, Conant LL. Where is the semantic system? A critical review and meta-analysis of 120 functional neuroimaging studies. Cereb Cortex 2009; 19: 2767–96.

Bozeat S, Lambon Ralph MA, Patterson K, Garrard P, Hodges JR. Non-verbal semantic impairment in semantic dementia. Neuropsychologia 2000; 38: 1207–15.

Brambati SM, Amici S, Racine CA, Neuhaus J, Miller Z, Ogar J, et al. Longitudinal gray matter contraction in three variants of primary progressive aphasia: a tenser-based morphometry study. Neuroimage Clin 2015; 8: 345–55.

Brambati SM, Rankin KP, Narvid J, Seeley WW, Dean D, Rosen HJ, et al. Atrophy progression in semantic dementia with asymmetric temporal involvement: a tensor-based morphometry study. Neurobiol Aging 2009; 30: 103–11.

Buckner RL, Andrews-Hanna JR, Schacter DL. The brain's default network: anatomy, function, and relevance to disease. Ann N Y Acad Sci 2008; 1124: 1–38.

Buckner RL, Sepulcre J, Talukdar T, Krienen FM, Liu H, Hedden T, et al. Cortical hubs revealed by intrinsic functional connectivity: mapping, assessment of stability, and relation to Alzheimer's disease. J Neurosci 2009; 29: 1860–73.

Buckner RL, Snyder AZ, Shannon BJ, Larossa G, Sachs R, Fotenos AF, et al. Molecular, structural, and functional characterization of Alzheimer's disease: evidence for a relationship between default activity, amyloid, and memory. J Neurosci 2005; 25: 7709–17.

Bullmore E, Sporns O. Complex brain networks: graph theoretical analysis of structural and functional systems. Nat Rev Neurosci 2009; 10: 186–98.

Butler CR, Brambati SM, Miller BL, Gorno-Tempini ML. The neural correlates of verbal and non-verbal semantic processing deficits in neurodegenerative disease. Cogn Behav Neurol 2009; 22: 73–80.

Catani M, Howard RJ, Pajevic S, Jones DK. Virtual *in Vivo* interactive dissection of white matter fasciculi in the human brain. Neuroimage 2002; 17: 77–94.

Catani M, Thiebaut De Schotten M. A diffusion tensor imaging tractography atlas for virtual *in vivo* dissections. Cortex 2008; 44: 1105–32.

Chan D, Anderson V, Pijnenburg Y, Whitwell J, Barnes J, Scahill R, et al. The clinical profile of right temporal lobe atrophy. Brain 2009; 132: 1287–98.

Chan D, Fox NC, Scahill RI, Crum WR, Whitwell JL, Leschziner G, et al. Patterns of temporal lobe atrophy in semantic dementia and Alzheimer's disease. Ann Neurol 2001; 49: 433–42.

Czarnecki K, Duffy JR, Nehl CR, Cross SA, Molano JR, Jack CR Jr, et al. Very early semantic dementia with progressive temporal lobe atrophy: an 8-year longitudinal study. Arch Neurol 2008; 65: 1659–63.

Dale AM, Fischl B, Serano MI. Cortical surface-based analysis. I. Segmentation and surface reconstruction. Neuroimage 1999; 9: 179–194.

Damasio H, Tranel D, Grabowski T, Adolphs R, Damasio A. Neural systems behind word and concept retrieval. Cognition 2004; 92: 179–229.

Davies RR, Halliday GM, Xuereb JH, Kril JJ, Hodges JR. The neural basis of semantic memory: evidence from semantic dementia. Neurobiol Aging 2009; 30: 2043–52.

Diehl-Schmid J, Onur OA, Kuhn J, Gruppe T, Drzezga A. Imaging frontotemporal lobar degeneration. Curr Neurol Neurosci Rep 2014; 14: 489–89.

Ding S-L, Van Hoesen GW, Cassell MD, Poremba A. Parcellation of human temporal polar cortex: a combined analysis of multiple cytoarchitectonic, chemoarchitectonic and pathological markers. J Comp Neurol 2009; 514: 595–623.

Englund E, Brun A, Alling C. White matter changes in dementia of Alzheimer's type. Biochemical and neuropathological correlates. Brain 1988; 111 (Pt 6): 1425–39.

Fischl B, Dale AM. Measuring the thickness of the human cerebral cortex from magnetic resonance images. Proc Natl Acad Sci USA 2000; 97: 11050–5.

Fischl B, Liu A, Dale AM. Automated manifold surgery: constructing geometrically accurate and topologically correct models of the human cerebral cortex. IEEE Trans Med Imaging 2001; 20: 70–80.

Fischl B, Sereno MI, Dale AM. Cortical surface-based analysis. II: inflation, flattening, and a surface-based coordinate system. Neuroimage 1999; 9: 195–207.

Frost B, Ollesch J, Wille H, Diamond MI. Conformational diversity of wild-type Tau fibrils specified by templated conformation change. J Biol Chem 2009; 284: 3546–51.

Gainotti G. The format of conceptual representations disrupted in semantic dementia: a position paper. Cortex 2012; 48: 521–9.

Gainotti G. Is the difference between right and left ATLs due to the distinction between general and social cognition or between verbal and non-verbal representations?. Neurosci Biobehav Rev 2015; 51: 296–312.

Galton CJ, Patterson K, Graham K, Lambon-Ralph MA, Williams G, Antoun N, et al. Differing patterns of temporal atrophy in Alzheimer's disease and semantic dementia. Neurology 2001; 57: 216–25.

Goll JC, Crutch SJ, Loo JHY, Rohrer JD, Frost C, Bamiou DE, et al. Non-verbal sound processing in the primary progressive aphasias. Brain 2010; 133: 272–85.

Gorno-Tempini ML, Dronkers NF, Rankin KP, Ogar JM, Phengrasamy L, Rosen HJ, et al. Cognition and anatomy in three variants of primary progressive aphasia. Ann Neurol 2004; 55: 335–46.

Gorno-Tempini ML, Hillis AE, Weintraub S, Kertesz A, Mendez M, Cappa SF, et al. Classification of primary progressive aphasia and its variants. Neurology 2011; 76: 1006–14.

Grothe MJ, Teipel SJ, Alzheimer's Disease Neuroimaging Initiative. Spatial patterns of atrophy, hypometabolism, and amyloid deposition in Alzheimer's disease correspond to dissociable functional brain networks. Hum Brain Mapp 2016; 37: 35–53.

Guo CC, Gorno-Tempini ML, Gesierich B, Henry M, Trujillo A, Shany-Ur T, et al. Anterior temporal lobe degeneration produces widespread network-driven dysfunction. Brain 2013; 136 (Pt 10): 2979–91.

Hermundstad AM, Bassett DS, Brown KS, Aminoff EM, Clewett D, Freeman S, et al. Structural foundations of resting-state and task-based functional connectivity in the human brain. Proc Natl Acad Sci USA 2013; 110: 6169–74.

Hodges JR, Bozeat S, Lambon Ralph MA, Patterson K, Spatt J. The role of conceptual knowledge in object use evidence from semantic dementia. Brain 2000; 123 (Pt 9): 1913–25.

Hodges JR, Mitchell J, Dawson K, Spillantini MG, Xuereb JH, Mcmonagle P, et al. Semantic dementia: demography, familial factors and survival in a consecutive series of 100 cases. Brain 2010; 133: 300–6.

Hodges JR, Patterson K. Semantic dementia: a unique clinicopathological syndrome. Lancet Neurol 2007; 6: 1004–14.

Hodges JR, Patterson K, Oxbury S, Funnell E. Semantic dementia. Brain 1992; 115: 1783–806.

Hoffman P, Jones RW, Ralph MaL. The degraded concept representation system in semantic dementia: damage to pan-modal hub, then visual spoke. Brain 2012; 135 (Pt 12): 3770–80.

Honey CJ, Sporns O, Cammoun L, Gigandet X, Thiran JP, Meuli R, et al. Predicting human resting-state functional connectivity. Proc Natl Acad Sci USA 2009; 106: 2035–40.

Hurley RS, Bonakdarpour B, Wang X, Mesulam MM. Asymmetric connectivity between the anterior temporal lobe and the language network. J Cogn Neurosci 2015; 27: 464–73.

Iaccarino L, Crespi C, Della Rosa PA, Catricala E, Guidi L, Marcone A, et al. The semantic variant of primary progressive aphasia: clinical and neuroimaging evidence in single subjects. PLoS One 2015; 10: e0120197.

Irish M, Hodges JR, Piguet O. Right anterior temporal lobe dysfunction underlies theory of mind impairments in semantic dementia. Brain 2014; 137 (Pt 4): 1241–53.

Irish M, Kumfor F, Hodges JR, Piguet O. A tale of two hemispheres: contrasting socioemotional dysfunction in right- versus left-lateralised semantic dementia. Dementia E Neuropsychologia 2013; 7: 88–95.

Josephs KA, Whitwell JL, Knopman DS, Boeve BF, Vemuri P, Senjem ML, et al. Two distinct subtypes of right temporal variant frontotemporal dementia. Neurology 2009; 73: 1443–50.

Kuczynski B, Targan E, Madison C, Weiner M, Zhang Y, Reed B, et al. White matter integrity and cortical metabolic associations in aging and dementia. Alzheimers Dement 2010; 6: 54–62.

La Joie R, Landeau B, Perrotin A, Bejanin A, Egret S, Pélerin A, et al. Intrinsic connectivity identifies the hippocampus as a main crossroad between Alzheimer's and semantic dementia-targeted networks. Neuron 2014; 81: 1417–28.

Lambon Ralph MA, Lowe C, Rogers TT. Neural basis of category-specific semantic deficits for living things: evidence from semantic dementia, HSVE and a neural network model. Brain 2007; 130: 1127–37.

Lambon Ralph MA, Sage K, Jones RW, Mayberry EJ. Coherent concepts are computed in the anterior temporal lobes. Proc Natl Acad Sci USA 2010; 107: 2717–22.

Luzzi S, Snowden JS, Neary D, Coccia M, Provinciali L, Lambon Ralph MA. Distinct patterns of olfactory impairment in Alzheimer's disease, semantic dementia, frontotemporal dementia, and corticobasal degeneration. Neuropsychologia 2007; 45: 1823–31.

Makris N, Meyer JW, Bates JF, Yeterian EH, Kennedy DN, Caviness VS. MRI-Based topographic parcellation of human cerebral white matter and nuclei II. Rationale and applications with systematics of cerebral connectivity. Neuroimage 1999; 9: 18–45.

Makris N, Papadimitriou GM, Kaiser JR, Sorg S, Kennedy DN, Pandya DN. Delineation of the middle longitudinal fascicle in humans: a quantitative, *in vivo*, DT-MRI study. Cereb Cortex 2009; 19: 777–85.

Makris N, Preti MG, Asami T, Pelavin P, Campbell B, Papadimitriou GM, et al. Human middle longitudinal fascicle: variations in patterns of anatomical connections. Brain Struct Funct 2013a; 218: 951–68.

Makris N, Preti MG, Wassermann D, Rathi Y, Papadimitriou GM, Yergatian C, et al. Human middle longitudinal fascicle: segregation and behavioral-clinical implications of two distinct fiber connections linking temporal pole and superior temporal gyrus with the angular gyrus or superior parietal lobule using multi-tensor tractography. Brain Imaging Behav 2013b; 7: 335–52.

Martin A. The representation of object concepts in the brain. Ann Rev Psychol 2007; 58: 25–45.

Mesulam MM. A plasticity-based theory of the pathogenesis of Alzheimer's disease. Ann N Y Acad Sci 2000; 924: 42–52.

Mesulam MM. Primary progressive aphasia-A language-based dementia. N Engl J Med 2003; 349: 1535–42.

Mesulam MM, Thompson CK, Weintraub S, Rogalski EJ. The wernicke conundrum and the anatomy of language comprehension in primary progressive aphasia. Brain 2015; 138 (Pt 8): 2423–37.

Mesulam MM, Wieneke C, Hurley R, Rademaker A, Thompson CK, Weintraub S, et al. Words and objects at the tip of the left temporal lobe in primary progressive aphasia. Brain 2013; 136: 601–18.

Miller ZA, Mandelli ML, Rankin KP, Henry ML, Babiak MC, Frazier DT, et al. Handedness and language learning disability

differentially distribute in progressive aphasia variants. Brain 2013; 136: 3461–73.
Mion M, Patterson K, Acosta-Cabronero J, Pengas G, Izquierdo-Garcia D, Hong YT, et al. What the left and right anterior fusiform gyri tell us about semantic memory. Brain 2010; 133: 3256–68.
Mueller S, Wang D, Fox MD, Yeo BTT, Sepulcre J, Sabuncu MR, et al. Individual variability in functional connectivity architecture of the human brain. Neuron 2013; 77: 586–95.
Mummery CJ, Patterson K, Price CJ, Ashburner J, Frackowiak RSJ, Hodges JR. A voxel-based morphometry study of semantic dementia: relationship between temporal lobe atrophy and semantic memory. Ann Neurol 2000; 47: 36–45.
Olson IR, Mccoy D, Klobusicky E, Ross LA. Social cognition and the anterior temporal lobes : a review and theoretical framework. Soc Cogn Affect Neurosci 2013; 8: 123–33.
Olson IR, Plotzker A, Ezzyat Y. The enigmatic temporal pole: a review of findings on social and emotional processing. Brain 2007; 130 (Pt 7): 1718–31.
Palop JJ, Mucke L. Amyloid-beta-induced neuronal dysfunction in Alzheimer's disease: from synapses toward neural networks. Nat Neurosci 2010; 13: 812–18.
Pascual B, Masdeu JC, Hollenbeck M, Makris N, Insausti R, Ding SL, et al. Large-scale brain networks of the human left temporal pole: a functional connectivity MRI study. Cereb Cortex 2015; 25: 680–702.
Patel MD, Toussaint N, Charles-Edwards GD, Lin JP, Batchelor PG. Distribution and fibre field similarity mapping of the human anterior commissure fibres by diffusion tensor imaging. Magma 2010; 23: 399–408.
Patterson K, Nestor PJ, Rogers TT. Where do you know what you know? The representation of semantic knowledge in the human brain. Nat Rev Neurosci 2007; 8: 976–87.
Piwnica Worms KE, Omar R, Hailstone JC, Warren JD. Flavour processing in semantic dementia. Cortex 2010; 46: 761–68.
Pyles JA, Verstynen TD, Schneider W, Tarr MJ. Explicating the face perception network with white matter connectivity. PLoS One 2013; 8: e61611–e11.
Raj A, Kuceyeski A, Weiner M. A network diffusion model of disease progression in dementia. Neuron 2012; 73: 1204–15.
Rice GE, Hoffman P, Lambon Ralph MA. Graded specialization within and between the anterior temporal lobes. Ann N Y Acad Sci 2015a; 1359: 84–97.
Rice GE, Lambon Ralph MA, Hoffman P. The roles of left versus right anterior temporal lobes in conceptual knowledge: an ALE meta-analysis of 97 functional neuroimaging studies. Cereb Cortex 2015b; 25: 4374–91.
Rogalski E, Cobia D, Harrison TM, Wieneke C, Weintraub S, Mesulam MM. Progression of language decline and cortical atrophy in subtypes of primary progressive aphasia. Neurology 2011; 76: 1804–10.
Rogalski E, Cobia D, Martersteck A, Rademaker A, Wieneke C, Weintraub S, et al. Asymmetry of cortical decline in subtypes of primary progressive aphasia. Neurology 2014; 83: 1184–91.
Rogalski E, Johnson N, Weintraub S, Mesulam M. Increased frequency of learning disability in patients with primary progressive aphasia and their first-degree relatives. Arch Neurol 2008; 65: 244–8.
Rohrer JD, Warren JD. Phenomenology and anatomy of abnormal behaviours in primary progressive aphasia. J Neurol Sci 2010; 293: 35–8.
Rohrer JD, Warren JD, Modat M, Ridgway GR, Douiri A, Rossor MN, et al. Patterns of cortical thinning in the language variants of frontotemporal lobar degeneration. Neurology 2009; 72: 1562–9.
Rosas HD, Liu AK, Hersch S, Glessner M, Ferrante RJ, Salat DH, et al. Regional and progressive thinning of the cortical ribbon in Huntington's disease. Neurology 2002; 58: 695–701.
Rosen HJ, Gorno-Tempini ML, Goldman WP, Perry RJ, Schuff N, Weiner M, et al. Patterns of brain atrophy in frontotemporal dementia and semantic dementia. Neurology 2002; 58: 198–208.
Salat DH, Buckner RL, Snyder AZ, Greve DN, Desikan RS, Busa E, et al. Thinning of the cerebral cortex in aging. Cerebral Cortex. Neuron 2004; 14: 721–730.
Sanders DW, Kaufman SK, Devos SL, Sharma AM, Mirbaha H, Li A, et al. Distinct tau prion strains propagate in cells and mice and define different tauopathies. Neuron 2014; 82: 1271–88.
Sapolsky D, Bakkour A, Negreira A, Nalipinski P, Weintraub S, Mesulam MM, et al. Cortical neuroanatomic correlates of symptom severity in primary progressive aphasia. Neurology 2010; 75: 358–66.
Seeley WW, Bauer AM, Miller BL, Gorno-Tempini ML, Kramer JH, Weiner M, et al. The natural history of temporal variant frontotemporal dementia. Neurology 2005; 64: 1384–90.
Seeley WW, Crawford RK, Zhou J, Miller BL, Greicius MD. Neurodegenerative diseases target large-scale human brain networks. Neuron 2009; 62: 42–52.
Sepulcre J, Sabuncu MR, Yeo TB, Liu H, Johnson KA. Stepwise connectivity of the modal cortex reveals the multimodal organization of the human brain. J Neurosci 2012; 32: 10649–61.
Simmons WK, Martin A. The anterior temporal lobes and the functional architecture of semantic memory. J Int Neuropsychol Soc 2009; 15: 645–9.
Snowden JS, Goulding PJ, Neary D. Semantic dementia : a form of circumscribed atrophy. Behav Neurol 1989; 2: 167–82.
Spreng RN, Rosen HJ, Strother S, Chow TW, Diehl-Schmid J, Freedman M, et al. Occupation attributes relate to location of atrophy in frontotemporal lobar degeneration. Neuropsychologia 2010; 48: 3634–41.
Van Den Heuvel MP, Mandl RCW, Kahn RS, Hulshoff Pol HE. Functionally linked resting-state networks reflect the underlying structural connectivity architecture of the human brain. Hum Brain Mapp 2009; 30: 3127–41.
Van Dijk KRA, Hedden T, Venkataraman A, Evans KC, Lazar SW, Buckner RL. Intrinsic functional connectivity as a tool for human connectomics: theory, properties, and optimization. J Neurophysiol 2010; 103: 297–321.
Villain N, Desgranges B, Viader F, De La Sayette V, Mézenge F, Landeau B, et al. Relationships between hippocampal atrophy, white matter disruption, and gray matter hypometabolism in Alzheimer's disease. J Neurosci 2008; 28: 6174–81.
Visser M, Jefferies E, Lambon Ralph MA. Semantic processing in the anterior temporal lobes: a meta-analysis of the functional neuroimaging literature. J Cogn Neurosci 2010; 22: 1083–94.
Warrington EK. The selective impairment of semantic memory. Q J Exp Psychol 1975; 27: 635–57.
Whitwell JL, Josephs KA. Recent advances in the imaging of frontotemporal dementia. Curr Neurol Neurosci Rep 2012; 12: 715–23.
Wilson SM, Demarco AT, Henry ML, Gesierich B, Babiak M, Mandelli ML, et al. What role does the anterior temporal lobe play in sentence-level processing? Neural correlates of syntactic processing in semantic PPA. J Cogn Neurosci 2014; 26: 970–85.
Winkler AM, Ridgway GR, Webster MA, Smith SM, Nichols TE. Permutation inference for the general linear model. Neuroimage 2014; 92: 381–97.
Wong C, Gallate J. The function of the anterior temporal lobe: a review of the empirical evidence. Brain Res 2012; 1449: 94–116.
Xie T, He Y. Mapping the Alzheimer's brain with connectomics. Front Psychiatry 2011; 2: 77.
Zhou J, Gennatas ED, Kramer JH, Miller BL, Seeley WW. Predicting regional neurodegeneration from the healthy brain functional connectome. Neuron 2012; 73: 1216–27.